Applied Catalysis B: Environmental 226 (2018) 585–595

Contents lists available at ScienceDirect

Applied Catalysis B: Environmental

journal homepage: www.elsevier.com/locate/apcatb

Boosting catalytic propane oxidation over PGM-free Co_3O_4 nanocrystal aggregates through chemical leaching: A comparative study with Pt and Pd based catalysts

Wenxiang Tang[a], Wen Xiao[b], Sibo Wang[a], Zheng Ren[a], Jun Ding[b], Pu-Xian Gao[a,*]

[a] Department of Materials Science and Engineering & Institute of Materials Science, University of Connecticut, Storrs, CT 06269-3136, USA
[b] Department of Materials Science & Engineering, National University of Singapore, Singapore 117574, Singapore

ARTICLE INFO

Keywords:
Cobalt oxide
Chemical leaching
Nanocatalyst
Propane oxidation
Surface chemistry

ABSTRACT

Rational modification of interfacial structure and chemistry can help effectively tailor the reactivity and stability of heterogeneous catalysts regardless of their elemental or compound natures. Herein, a diluted acidic treatment was designed and utilized to modify the surface structure and chemistry of spinel Co_3O_4 nanoparticles. Such a chemical leaching strategy has significantly promoted the propane oxidation activity of the PGM-free Co_3O_4 nanocrystal aggregates. With a much higher activity than the commercial Al_2O_3 supported Pt and Pd catalysts, these leached nanoparticle aggregates exhibited much more abundant defects, surface Co^{2+} and chemisorbed oxygen species. Such surface-modified Co_3O_4 nanocatalysts have displayed excellent and stable propane oxidation efficiency independent of both O_2 and C_3H_8 concentrations, where the activities of both commercial Pt (or Pd)/Al_2O_3 and self-made Pt (or Pd)/CeO_2 catalysts were greatly affected by different O_2 and C_3H_8 concentrations. Meanwhile, the Co_3O_4 nanocrystal aggregates catalyst exhibited good performance in presence of water or sulfur dioxide. This facile chemical leaching based technique provides a potential means to make highly active and stable oxide catalysts.

1. Introduction

Hydrocarbons (HCs) is a major group of atmospheric pollutants emitted from both mobile and stationary combustion sources such as fossil-fueled engines, petrochemical processes, industrial and power plants, and the treatment of solid and liquid wastes [1,2]. Due to their high activities while interacting with NO_x and ozone, HCs can induce the formation of toxic ozone and photo-smog, and are a major family of greenhouse gases leading to global warming [3,4]. Due to the wide usage of liquefied petroleum gas (LPG), primarily composed of propane and butane, and compressed natural gas (CNG) such as methane as fuel sources, more and more attention has been given to the release of light alkanes, the largest fraction of exhaust especially from low-temperature combustion (LTC) engines [5,6]. In addition, more and more light alkanes are also emitted from stationary sources due to the intensive development and deployment of various chemical processes. Therefore, controlling the light alkane emissions is a very important pollution control task in the future. Amongst the few available technologies for hydrocarbons emissions abatement, such as condensation-recycling, adsorption and fuel-assisted combustion, catalytic oxidation is considered the most efficient means especially under low gas concentration and at low operating temperatures [7,8].

Supported platinum group metal (PGM) (such as Pt, Pd, Rh, Ru and Au) catalysts are commonly used for catalytic total oxidation of hydrocarbons with good activities [7,9,10]. Some of them such as three-way catalyst (TWC) and diesel oxidation catalyst (DOC) have been used to control CO and hydrocarbon emissions, however, there are still some drawbacks such as high price, low availability, sintering issue, and susceptibly poisoning tendency [7,8]. Recently, O'Brien et al. [11] reported that, with the varying of O_2/C_3H_8 ratio, the conversion of propane was greatly affected even at higher temperature and reached a maximum at an O_2/C_3H_8 ratio of 4. Such a problem might be a common issue in PGM catalysts for hydrocarbon combustion and therefore developing novel catalysts to overcome this critical issue are highly desirable. For catalytic light alkane oxidation, some low-cost PGM-free metal oxide catalysts such as Co_3O_4 [12–14], MnO_2 [15,16], CeO_2 [17,18], Co−Ce−O [19,20], Mn−Co−O [21] and perovskite [22,23] have been proved to be active and have great potential for replacing the PGM based catalyst. However, these metal oxide catalysts usually are less active than the PGM based catalysts.

Recently, Li et al. have applied selective chemical etching method to treat three dimensional chain-like ordered microporous (3DOM) ABO_3-

* Corresponding author.
E-mail address: puxian.gao@uconn.edu (P.-X. Gao).

https://doi.org/10.1016/j.apcatb.2017.12.075
Received 28 September 2017; Received in revised form 22 December 2017; Accepted 31 December 2017
Available online 01 January 2018

type perovskite to create modified nanomaterials with much higher catalytic activities such as SD-LMO [24], MnO_2/LMO [25], γ-MnO_2 [26], $La_{1-x}Sr_xCoO_3$ [27]. By controlling acidic treatment process, A-site cations such as lanthanum in the perovskite structures can be selectively removed to form new materials with high meoporosity, excellent low-temperature reducibility, and improved surface defective oxygen species, which can all contribute to the promoted performance. Co_3O_4, a classical low-cost transition metal oxide, has a spinel crystal structure with tetrahedral-site-occupied Co^{2+} and octahedral-site-occupied Co^{3+}. It has been widely reported as a potential catalyst for catalyzing different oxidations such as CO oxidation, hydrocarbon combustions and NO oxidation [12,28–31]. However, the activity of bulk material is usually poor. Some research has demonstrated that the activity of Co_3O_4 could be improved by decreasing particle size [12], increasing specific surface area [30,31], and selectively exposing lattice planes [29] etc. Importantly, the surface chemistry-environment plays a vital role in catalytic reactions so directly controlling the surface structure of catalyst will has great potential in boosting the activity of catalyst particles. Here in our work, the chemical leaching strategy was firstly used for treating Co_3O_4 nanomaterial and the activity in propane combustion could be significantly promoted, as well as a much higher than the commercial Al_2O_3 and CeO_2 supported PGM (e.g., Pt and Pd) catalysts. Evidently the chemical leaching greatly modified the surface chemistry like surface defects, surface Co^{2+} species, and chemisorbed oxygen species, as well as oxygen mobility. Such surface-modified Co_3O_4 nanocatslyst have displayed an excellent and stable propane conversion efficiency independent of both O_2 and C_3H_8 concentrations, where the activities of commercial noble-metal based catalysts such as Pt (or Pd)/Al_2O_3 and Pt (or Pd)/CeO_2 would be greatly affected by different O_2 and C_3H_8 concentrations. This facile chemical leaching based technique provides a potential means to make highly active and stable oxide catalysts in replacement of now used platinum group metal (PGM) based catalysts.

2. Experimental

2.1. Materials preparation

2.1.1. Preparation of porous Co_3O nanoparticles

A simple modified oxalate route was used to synthesize the cobalt oxalate precursors in an aqueous solution, which was further annealed in air to get the porous Co_3O_4 nanoparticles. In a typical synthesis, two aqueous solutions, $Co(NO_3)_2$ (20 mmol, 80 ml) and $Na_2C_2O_4$ (30 mmol, 120 ml), respectively, were heated at 80 °C for 15 min, then mixed under strong stirring. The precipitation reaction occurred in a few seconds and the mixture was stirred for another 0.5 h at 80 °C. Finally, the precipitate was filtered, washed and dried at 80 °C overnight, followed by thermal treatment at 500 °C for 2 h with a ramp rate of 5 °C min^{-1} under ambient atmosphere. These as-prepared Co_3O_4 particles were labeled as Co_3O_4-original.

2.1.2. Chemical etching by acetic acid

A dilute acetic acid was selected for the chemical etching treatment. Typically, 500 mg Co_3O_4-orignial powder was added into 100 ml of 0.1 M acetic acid solution at 60 °C. The suspension was vigorously stirred for 1 h, then filtered and washed with deionized water until the pH was neutral, followed by drying at 150 °C overnight. The sample achieved after chemical etching was labeled as Co_3O_4-AC.

2.1.3. Commercial Pt/Al_2O_3 and Pd/Al_2O_3 powders

Two commercial catalysts (1 wt.%Pt/Al_2O_3 and 1 wt.%Pd/Al_2O_3) purchased from Sigma-Aldrich were also tested for comparison. Before test, the commercial powder was treated at 500 °C for 2 h with a ramp rate of 5 °C min^{-1} under ambient condition. The TEM results (as shown in Figs. S1 and S2) showed the Pt/Al_2O_3 had two kinds of Pt particle sizes: one is about 10 nm, the other is below 2 nm. The Pd size of Pd/Al_2O_3 is about 2–5 nm.

2.1.4. Self-made Pt/CeO_2 and Pd/CeO_2

Wet impregnation method was applied for loading Pt or Pd nanoparticles on commercial CeO_2 nanoparticles. Typically, a certain Pt or Pd precursor (chloroplatinic acid or ammonium tetrachloropalladate (II)) was dissolved into water and then add CeO_2 powder. The mixture was sonicated for 1 h and dried at 80 °C for 6 h. Finally, the 1 wt.% Pt/CeO_2 and 1 wt.% Pd/CeO_2 were achieved by annealing the dried samples at 500 °C for 2 h with a ramp rate of 5 °C min^{-1} under ambient condition. The TEM results (as shown in Fig. S1) showed the size of both Pt and Pd on CeO_2 is about 2–5 nm.

2.2. Materials characterization

A D2 pH ASER X-ray diffractometer system (BRUKER Corp., USA) was used to record the X-ray diffraction (XRD) patterns of as-prepared samples with a 2θ scanning rate of 0.3° min^{-1}. Raman spectra were acquired on a Reinshaw 2000 Ramascope with a CCD camera and an Ar^+ laser (514.4 nm) as the excitation source. The structural properties were measured using a N_2 adsorption-desorption method at liquid nitrogen temperature, which was carried out on an ASAP 2020 volumetric adsorption analyzer from Micromeritics Instrument Corp. Each sample was degassed under vacuum at 150 °C for 6 h before measurement. Surface area of each sample was determined by the Brunauer-Emmett-Teller (BET) plot of nitrogen adsorption data and the Barrett-Joyner-Halenda (BJH) method was used to calculate the pore size distribution. The morphology and microstructure of as-prepared catalysts were characterized on a scanning electron microscope (SEM, Teneo LVSEM, FEI, USA) and a scanning transmission electron microscope (TEM, Talos S/TEM, FEI, USA), respectively. X-ray photoelectron spectroscopy (XPS) was performed with a Kratos Analytical (Axis Ultra DLD) instrument equipped with monochromatic Al Ksource operating at 1486.7 eV. The signal was filtered with a hemispherical analyzer (pass energy 160 eV for survey spectra and 20 eV for narrow high-resolution scans). The C 1s photoelectron line at 284.6 eV was used as an internal standard for correction of charging effects in all samples. Hydrogen temperature programmed reduction (H_2-TPR) and oxygen temperature programmed desorption (O_2-TPD) were carried out in a U-shaped quartz reactor under a gas flow of 5% H_2 balanced with Ar for H_2-TPR and pure Ar for O_2-TPD, 25 ml min^{-1} on a Chemisorption system (ChemiSorb 2720, Micromeritics Cor.). Before doing the H_2-TPR analysis, the tested samples were purged under pure argon at 100 °C for 2 h, and cooled down to 50 °C. Before doing the O_2-TPD analysis, the tested samples were pretreated under oxygen atmosphere at 200 °C for 2 h, and cooled down to 50 °C then purged with pure argon gas. In every run, the temperature was ramped to 800 °C from 50 °C at a rate of 10 °C min^{-1}.

2.3. Catalytic test

Catalytic propane combustion was measured using a fixed bed micro-reactor in BechCAT system (Altamira Instruments, USA). For each test, 25 mg of powdered catalyst was placed in a ¼" o.d. quartz reactor tube with quartz wool sealed on both sides. Generally, the feed gas was mixed with 10 ml min^{-1} 3% C_3H_8, 10 ml min^{-1} O_2 and 80 ml min^{-1} N_2 (3000 ppm C_3H_8, 10% O_2 and 89.7% N_2) with a total flow rate of 100 ml min^{-1}, which gives a high weight hourly space velocity (WHSV) of 240 000 ml g^{-1} h^{-1}. The inlet and outlet gas species (C_3H_8, CO and CO_2) were detected by an Agilent Micro-GC gas analyzer (3000A or 490) equipped with two columns and two TCD detectors. The catalyst temperature was controlled by a K-type thermocouple positioned inside the middle of furnace and a thermometer was located in the reactor for monitoring the catalyst bed temperature on-line. During the C_3H_8 oxidation test, 24 temperature points in the range of 100–500 °C will be set and each point will be kept for 0.5 h to

reach a steady state. Notably, propane was completely oxidized to CO_2 and H_2O over the catalysts used in this study, and no partial oxidation products were found, as the carbon balance was maintained above 99.5%.

2.4. Stability test, water resistance and sulfur resistance

Cycling and time-on-stream test were used to evaluate the stability of as-prepared Co_3O_4-AC catalyst. For the five cycling experiments, the temperature is increased to 350 °C, and then cooled to room temperature during each cycle, with the feed gas controlled at 3000 ppm C_3H_8, 10% O_2 and 89.7% N_2 with a total flow rate of 100 ml min^{-1}, which gives a high weight hourly space velocity (WHSV) of 240 000 ml g^{-1} h^{-1}. The time-on-stream test was carried out at 280 °C for 60 h under the same feed gas condition. Hydrothermal treatment on Co_3O_4-Original and Co_3O_4-AC was operated at 700 °C for 50 h under gas composition of 10% CO_2, 10% H_2O, 10% O_2 and N_2 balanced. For water resistance test, about 3.0% water vapor was introduced into the reaction gas by bubbling water at room temperature (25 °C) and the performance test was operated at 280 °C for 6 h without water, then 6 h with 3.0% water vapor, finally 6 h without water. The investigation on effect of sulfur was carried out as the water-resistance test and 5 ppm SO_2 was introduced during the second 6h-running.

2.5. Effects of oxygen and propane concentration

To investigate the effects of oxygen and propane concentration on the catalytic activities, the propane oxidation experiments were performed isothermally under similar condition except variable oxygen or propane concentrations. The oxygen concentration varied from 2% to 50% while the propane concentration is 0.3%, which gives an O_2/C_3H_8 ratio from 6.67 to 166.7. The propane concentration varied from 0.06 to 1.5 while the O_2 concentration was 10%, giving the O_2/C_3H_8 ratio controlled from 166.7 to 6.67. Every step was maintained for 1 h to reach a steady state. As a comparison, both commercial Pt (or Pd)/Al_2O_3 and self-made Pt (or Pd)/CeO_2 catalysts were tested under the similar protocols. The temperatures used in these tests are 260 °C for Co_3O_4-AC, 400 °C for commercial 1%Pt/Al_2O_3 and self-made Pt (or Pd)/CeO_2, and 300 °C for commercial 1%Pd/Al_2O_3, respectively.

3. Results and discussion

3.1. Catalytic performance

Blank experiments without catalyst were carried out in an empty reactor which showed no significant conversion of propane even at 400 °C, demonstrating that no homogeneous reactions took place under the adopted reaction conditions. The catalytic activity of the original Co_3O_4 for propane total oxidation is presented in Fig. 1a. The propane combustion activity increased with raising reaction temperature, and the complete conversion of propane can be achieved at above 400 °C under lower WHSV of 60 000 ml g^{-1} h^{-1}. With increasing the WHSV to 240 000 ml g^{-1} h^{-1}, the performance is clearly inhibited where the complete converted temperature is high to 450 °C, which might be due to the reduction of contact time. It is true that catalytic activity could be decreased by increasing the WHSV (or SV), which has been reported in lots of studies especially the catalytic performances over oxides based catalysts [32–34]. Importantly, this will be a critical issue for the further application in practical hash environment so enhancing the activity at high WHSV will be highly desirable. With diluted acetic acid treatment, the Co_3O_4-AC showed a much better performance even at a very high WHSV of 240 000 ml g^{-1} h^{-1}, as shown in Fig. 1b. The reaction temperatures corresponding to the toluene conversion of 10%, 50% and 90% (T_{10}, T_{50}, T_{90}) were used to compare the catalytic activities of the samples, which are listed in Table 1. For the Co_3O_4-AC, the values of T_{50} and T_{90} are 235 and 250 °C, which are 105 and 150 °C lower than that over the original Co_3O_4 catalyst, respectively. Under the same condition, the commercial 1%Pd/Al_2O_3 showed much better performance in propane oxidation than the commercial 1%Pt/Al_2O_3 and self-made Pt (or Pd)/CeO_2, indicating Pd/Al_2O_3 based commercial catalyst is more efficient for propane combustion reaction. However, the activity of as-prepared Co_3O_4-original is still better than that over commercial 1%Pt/Al_2O_3 while it is worse than that of commercial 1%Pd/Al_2O_3 catalyst. But after a simple acid treated process, the activity of Co_3O_4-AC can be significantly boosted to a higher level, while the values of T_{50} and T_{90} are even 55 and 85 °C lower than that over the commercial 1%Pd/Al_2O_3 catalyst, respectively. As listed in Table 1, most of WHSV used in other reported literatures are below 60 000 ml g^{-1} h^{-1}, which is much lower than that used in our test. With lower WHSV (more catalyst usage or lower gas flow rate), the conversion temperature of propane can be achieved at a lower value, but this would be limited in the practical applications. In this study, even at high WHSV, the light-off temperature of Co_3O_4-AC is still comparable to that of other non-precious metal oxides based catalysts.

As shown in Fig. 2a and b, a cycling test and a time-on-stream test were carried out to study the stability of as-prepared Co_3O_4-AC. In order to investigate its catalytic stability, the test was performed five cycles under the same conditions, and in each cycle, the temperature is increased to 350 °C then cooled to room temperature. Significantly, no difference about the character of light-off curve was observed even after 5 cycling tests, indicating the acid treated Co_3O_4 has a superior catalytic stability for propane combustion at high WHSV. Moreover, the evolutions with time-on-stream of propane combustion over Co_3O_4-AC at 280 °C and 1%Pd/Al_2O_3 at 280 °C are completed for 60 h as shown in Fig. 2b. For commercial 1%Pd/Al_2O_3, the propane conversion decreased from 98% to 89% in 10 h, then slightly decreased during the

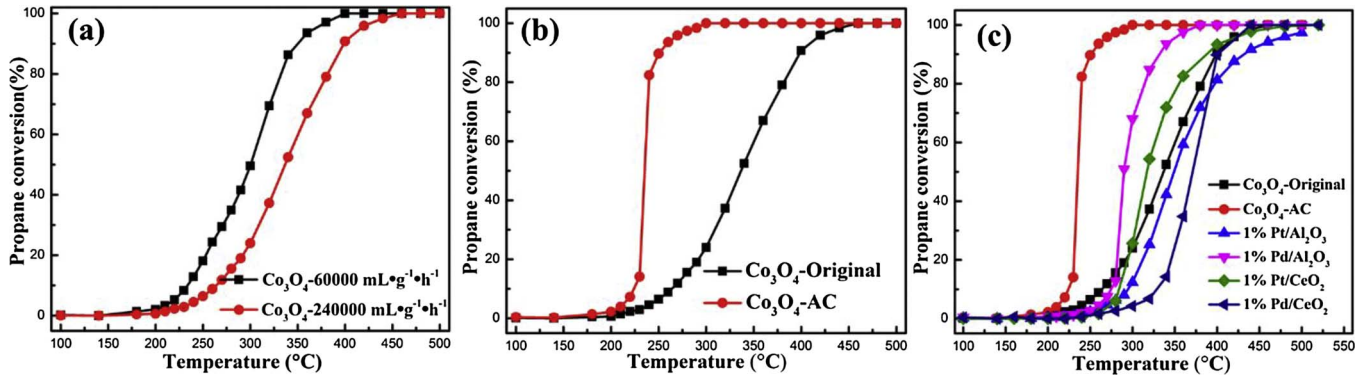

Fig. 1. (a) Catalytic combustion of propane (0.3% C_3H_8, 10% O_2 and N_2 balanced) as a function of temperature over (b) as-prepared original Co_3O_4 catalyst at different WHSV (60 000 and 240 000 ml g^{-1} h^{-1}); (c) as-prepared original Co_3O_4 catalyst and acetic acid treated Co_3O_4; (c) Co_3O_4, commercial 1%Pt/Al_2O_3 and 1%Pd/Al_2O_3, self-made 1%Pt/CeO_2 and 1%Pd/CeO_2, at WHSV of 240 000 ml g^{-1} h^{-1}.

Table 1
Catalytic testing condition (catalyst usage, flow rate, WHSV and propane concentration) and catalytic activities (T_{10}, T_{50}, T_{90}) of the as-prepared Co_3O_4 catalysts and other reported catalysts.

Catalyst	Catalyst usage (mg)	Flow rate (ml min^{-1})	WHSV (ml g^{-1} h^{-1})	C_3H_8 concentration (ppm)	T_{10} (°C)	T_{50} (°C)	T_{90} (°C)	Reference
Co_3O_4-original	100	100	60 000	3000	234	300	350	This study
Co_3O_4-original	25	100	240 000	3000	225	340	400	This study
Co_3O_4-AC	25	100	240 000	3000	224	235	250	This study
Commercial Pt/Al_2O_3	25	100	240 000	3000	295	350	432	This study
Commercial $PdAl_2O_3$	25	100	240 000	3000	275	290	335	This study
Self-made Pt/CeO_2	25	100	240 000	3000	284	318	389	This study
Self-made Pt/CeO_2	25	100	240 000	3000	330	371	401	This study
Co_3O_4	250	50	12 000	8000	220	250	280	[35]
Co_3O_4	100	50	30 000	5000	200	230	270	[36]
Co_3O_4	200	100	30 000	10 000	182	203	220	[37]
Co_3O_4	250	50	12 000	8000	170	205	212	[38]
Co_3O_4	50	100	120 000	1000	150	200	225	[39]
Co_3O_4/SiO_2	100	50	30 000	1000	240	280	320	[40]
Co_3O_4/ZSM-5	200	100	30 000	2000	205	235	260	[12]
$Ni_{0.5}Co_{0.5}Sc_xFe_{2-x}O_4$	300	100	20 000	10 000	180	240	400	[41]
$Co_xMn_{3-x}O_4$	50	97.8	117 360	4000	180	195	230	[42]
$MnNiO_x$	200	100	30 000	2000	186	215	242	[15]
La-MnO_x	200	100	30 000	2000	142	207	255	[43]

last 50 h. While for Co_3O_4-AC, during the 60 h of measurement, the conversion maintained at 100% without any deactivation, further demonstrating that this acid treated cobalt oxide catalyst performs an ultra-stable catalytic activity for propane oxidation and has great potential for practical applications. For practical application, water or SO_2 may have a negative effect on catalytic oxidation reactions. We introduced 3.0% water or 5 ppm SO_2 into the testing gas and the results are shown in Fig. 2. As we can see, at 280 °C, the conversion of propane can keep in 100% for long time when introduce either 3.0% water or 5 ppm SO_2. Therefore, this catalyst has a very good water/sulfur-resistance property. Moreover, the catalytic performance was also investigated after high-temperature hydrothermal treatment with the results displayed in Fig. S3. With high-temperature hydrothermal treatment, the light-off temperature of both Co_3O_4-original-HA and

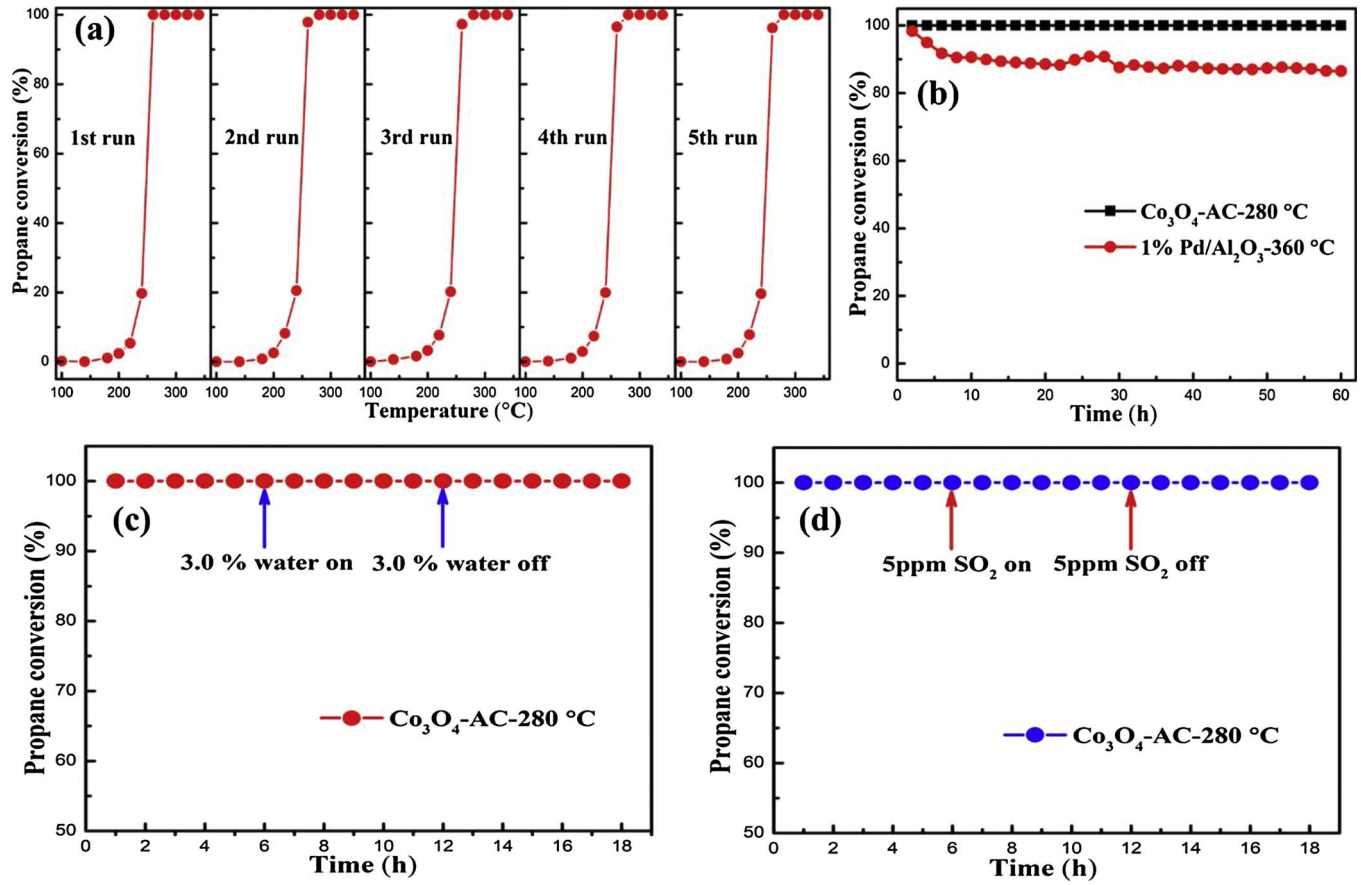

Fig. 2. (a) Cycling test of propane oxidation (0.3% C_3H_8, 10% O_2 and N_2 balanced) over the as-prepared Co_3O_4-AC catalyst at WHSV of 240 000 ml g^{-1} h^{-1}; (b) Catalytic combustion of propane oxidation (0.3% C_3H_8, 10% O_2 and N_2 balanced) over catalyst Co_3O_4-AC at 280 °C and commercial 1%Pd/Al_2O_3 at 360 °C for 60 h on stream at WHSV of 240 000 ml g^{-1} h^{-1}; (c) and (d) Catalytic combustion of propane oxidation (0.3% C_3H_8, 10% O_2 and N_2 balanced) over catalyst Co_3O_4-AC at 280 °C with/without introducing 3.0% water and 5 ppm SO_2 at WHSV of 240 000 ml g^{-1} h^{-1}.

Co_3O_4-AC-HA markedly increase while the complete conversion cannot be achieved below 500 °C. However, the Co_3O_4-AC-HA can still convert propane completely below 400 °C which is even better than the original Co_3O_4 catalyst.

In the practical gas exhaust, the concentrations of propane and oxygen as well as their ratios are varied during the emission process. Over noble metal based catalysts, the reaction gas atmosphere has a significant effect on the oxygen coverage and metal oxidation states of the noble nanoparticle, thus affecting the various catalytic activities in CO oxidation, HCs combustion [44,45]. Recently, O'Brien et al. [11] made an investigation on the kinetics of propane oxidation over Pt/Al_2O_3 as a function of O_2/C_3H_8 ratio in a temperature range of 150–300 °C. It was observed that the propane conversion increased with the O_2/C_3H_8 ratio until the conversion reached a maximum value at an O_2/C_3H_8 ratio of 4, and after that the conversion would decrease with increasing O_2/C_3H_8 ratio, which indicated a kinetic regime change from positive-order to negative-order with respect to the oxygen partial pressure. In our experiment, the ratio of O_2/C_3H_8 ranges from 6.67 to 166.7 with varying concentration of either oxygen or propane. For commercial $1\%Pt/Al_2O_3$ catalyst, the propane conversion decreases with increasing O_2 concentration, demonstrating a negative reaction order with respect to oxygen partial pressures, until the conversion keeps constant at above 30% O_2, as shown in Fig. 3a and b. Meanwhile, under maintained O_2 concentration, the propane conversion increases with increasing propane concentration as displayed in Fig. 3c and d. Through changing either the concentration of O_2 or C_3H_8, propane conversion displays a negative reaction order with respect to the ratio of O_2/C_3H_8, which is consistent with O'Brien's study [11]. In commercial $1\%Pd/Al_2O_3$ catalyst, the results are different as shown in Fig. 3. With increasing O_2 concentration, the propane conversion increased, which might be due to the formation of Pd-O species under O_2-rich atmosphere. Over Pd based oxidation catalysts, the Pd-O species have been claimed to make a great contribution on the catalytic oxidation reactions [10,46,47]. However, the result is very different with changing propane concentration, even the O_2/C_3H_8 ratio is in the same range under constant oxygen concentration. With increasing propane concentration, the conversion decreases until it reached a minimum (18%) at 0.3% propane (O_2/C_3H_8 = 33.3). After that, the conversion directly goes to a high level above 80% and keeps increasing when the propane concentration is increased. Compared to Al_2O_3, CeO_2 is supposed to be a better redox-oxygen cycling catalyst when used as a PGM support. However, in terms of propane oxidation, the performance of $1\%Pt/CeO_2$ and $1\%Pd/CeO_2$ are both greatly affected by the concentration of propane and oxygen, which is similar to the Al_2O_3

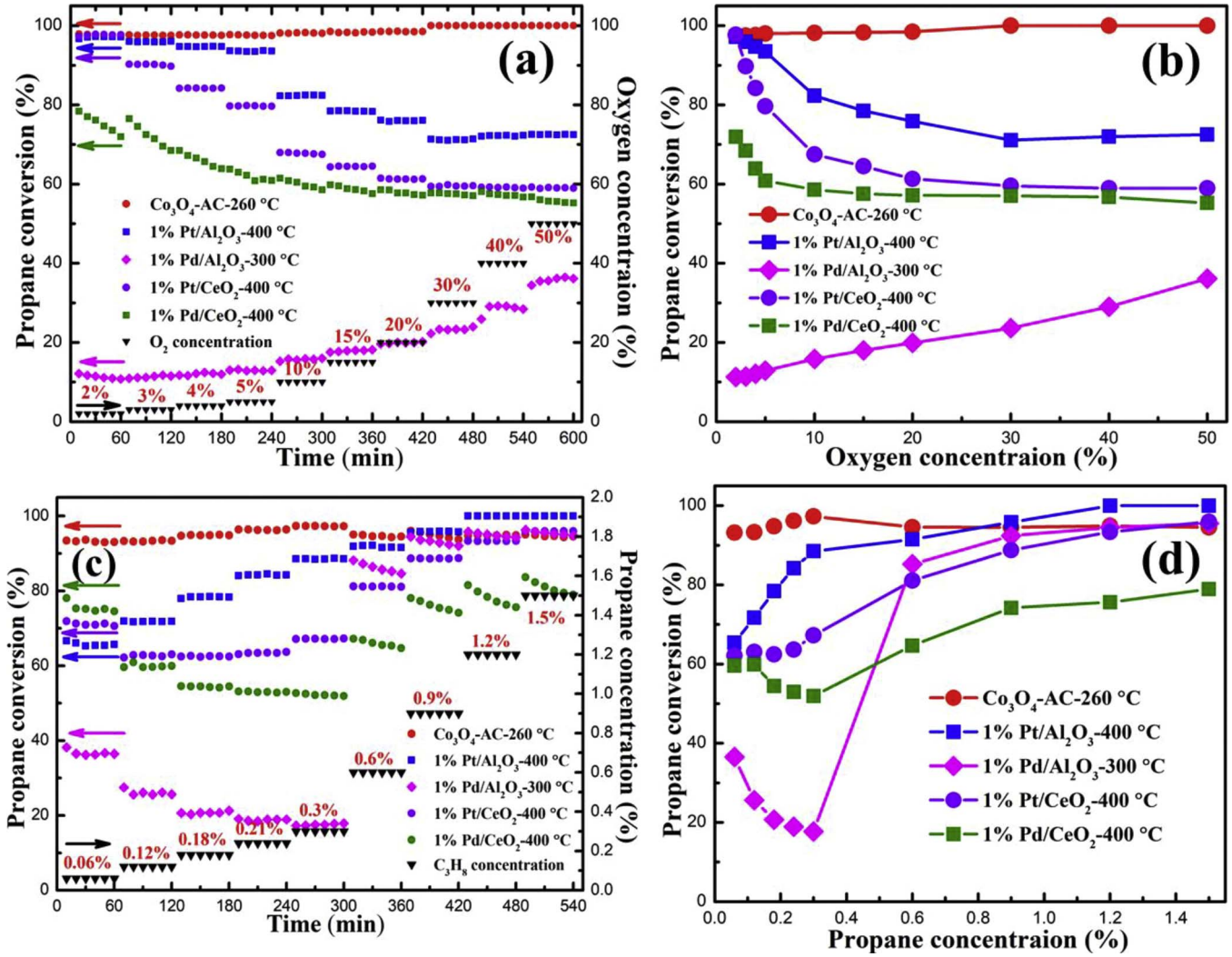

Fig. 3. The effect of oxygen concentration (2, 3, 4, 5, 10, 15, 20, 30, 40 and 50%) on the catalytic propane oxidation (0.3% C_3H_8 and N_2 balanced) activities over catalyst Co_3O_4-AC, commercial $1\%Pt/Al_2O_3$ and $1\%Pd/Al_2O_3$ at WHSV of 240 000 ml g^{-1} h^{-1}. (a) Propane conversion versus time with different concentration of O_2 feed; (b) propane conversion versus oxygen concentration. The effect of propane concentration (0.06, 0.12, 0.18, 0.24, 0.3, 0.6, 0.9, 1.2 and 1.5%) on the catalytic propane oxidation (10% O_2 and N_2 balanced) activities over catalyst Co_3O_4-AC, commercial $1\%Pt/Al_2O_3$, $1\%Pd/Al_2O_3$, self-made $1\%Pt/CeO_2$ and $1\%Pd/CeO_2$, at WHSV of 240 000 ml g^{-1} h^{-1}. (c) Propane conversion versus time with different concentration of C_3H_8 feed; (d) propane conversion versus C_3H_8 concentration.

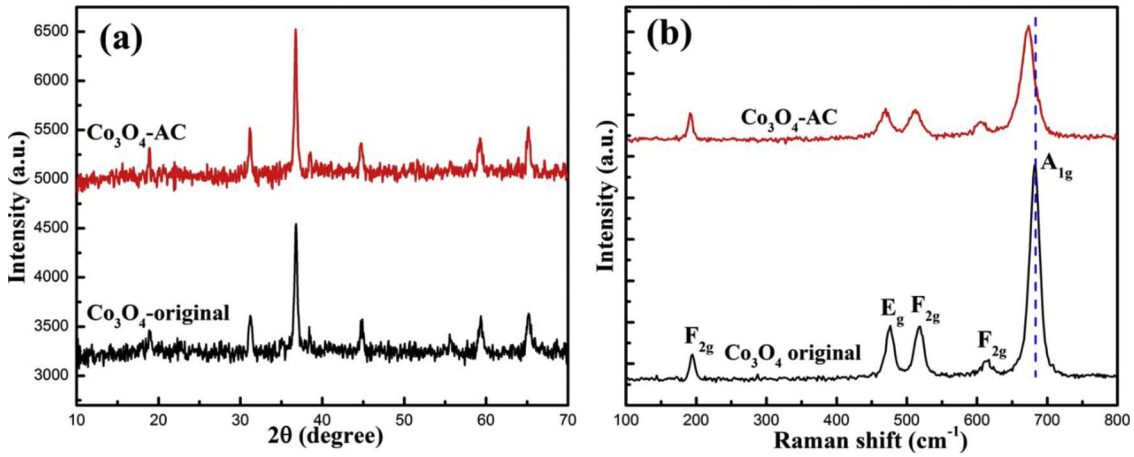

Fig. 4. (a) XRD and (b) Raman spectra patterns of the Co_3O_4-original and Co_3O_4-AC catalysts.

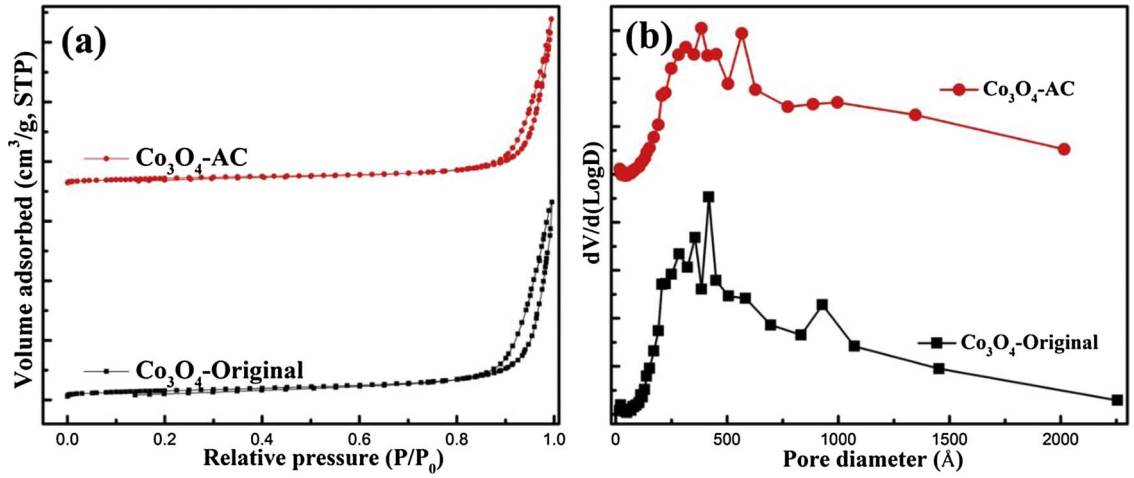

Fig. 5. (a) N_2 adsorption-desorption and (b) pore size distribution of the Co_3O_4-original and Co_3O_4-AC catalysts.

supported Pt and Pd catalysts. The reason for this unusual revolution is still unknown and more investigation on this will be desirable in the future. For the Co_3O_4-AC catalyst, the activity for propane oxidation highly independent under varied O_2/C_3H_8 ratio even at lower temperature compared to the Pt and Pd based catalysts. Especially at different oxygen concentration, the conversion can keep at above 98% and will slightly increase to 100% with increasing the oxygen concentration. As shown in Fig. 3c and d, the propane conversion firstly increases slightly with increasing propane concentration, until the propane concentration exceeds 0.3%. Under higher propane concentration, the conversion slowly decreases to a constant value while it is still above 90%. As a result, the Co_3O_4-AC catalyst has a versatile ability to be highly active at variable oxygen and propane concentrations, as well as low reaction temperature, which holds a great potential in practical applications.

3.2. Textural characterization of the catalysts

XRD, Raman spectra, N_2-physisorption, SEM and TEM were used to characterize the textural properties of as-prepared Co_3O_4-original and Co_3O_4-AC catalysts. Fig. 4a and b display the wide-angle XRD patterns and Raman spectra of the samples, respectively. From XRD patterns, the diffraction peaks at $2\theta = 18.8$, 31.2, 36.8, 38.5, 44.8, 59.2 and 65.1° can be clearly observed which are corresponded to the (111), (220), (311), (222), (400), (511) and (440) planes of spinel Co_3O_4 (JCPDS 78-1969). With diluted acid treatment, the final powder is still crystalline Co_3O_4 with spinel type structure and no obvious difference has been found from the XRD pattern. However, the cell parameter of Co_3O_4-original and Co_3O_4-AC are $a_0 = 8.093$ Å and 8.101 Å, respectively, which are achived by unit cell refinement analysis with HighScore Plus. With acidic treatment, the occurring of lattice expansion might due to the formation of defects in original electronic and geometric structure of Co_3O_4 [48,49]. Meanwhile, the crystallite size of Co_3O_4-AC (18.8 nm) was smaller than that of original Co_3O_4 (22.1 nm) calculated from the Scherrer Equation, which implied the Co_3O_4 nanoparticles were slightly dissolved by the acidic treatment. In Raman spectra, the peaks correspond to $F_{2g}^{(1)}$, E_g, $F_{2g}^{(2)}$, $F_{2g}^{(3)}$ and A_{1g} symmetries of Co_3O_4 can be obviously found at 195, 477, 519, 616 and 684 cm^{-1}, respectively. It can be seen that the acid treatment has a great effect on the Raman spectra of cobalt oxide. For instance, the A1 g of Co_3O_4-AC is located at about 673 cm^{-1} which is much lower than that of original Co_3O_4 (684 cm^{-1}). This clear red shift (~13 cm^{-1}) demonstrates that more defects like lattice distortion and residual stress of the spinel crystal were formed during the acid treatment process [37,50,51]. Meanwhile, the peak area ratios F2g/Eg (octahedral/tetrahedral site oxygen motions) of Co_3O_4-original and Co_3O_4-AC are 1.77 and 2.29, respectively. Theoretically, more lattice defects will generate more active sites like oxygen vacancies which will greatly enhance the activities of oxide based catalysts.

Fig. 5 shows the N_2 adsorption-desorption isotherm and pore size distribution patterns of the as-prepared Co_3O_4 catalysts. The result of N_2 physisorption reveals a typical H3-type hysteresis loops in the range of 0.8-1.0 relative pressure that is associated with the classical capillary condensation in mesopores, indicating the presence of mesoporous

Table 2
Physical and Chemical Parameters of the as-prepared Co_3O_4 catalysts.

Catalyst	BET			Surface species						H_2 consumption (mmol g^{-1})	
	Surface area ($m^2 g^{-1}$)	Pore diameter (nm)	Pore volume ($cm^3 g^{-1}$)	O_α (%)	O_β (%)	O_β/O_α	Co^{2+} (%)	Co^{3+} (%)	Co^{2+}/Co^{3+}	< 350 °C	350–500 °C
Co_3O_4-Original	27.90	28.79	0.26	59.4	32.6	0.549	31.2	68.8	0.45	2.33	14.0
Co_3O_4-AC	22.31	32.37	0.22	50.39	42.1	0.835	59.0	41.0	1.44	3.31	13.7

structure in the catalytic Co_3O_4 [50]. As listed in Table 2, the BET surface area is about 27.9 $m^2 g^{-1}$ while the value of Co_3O_4 after acidic treatment decreases to 22.31 $m^2 g^{-1}$. With acidic treatment, the porous structure of material keeps well according to the similar character of N_2 adsorption-desorption isotherm. Furthermore, the pore size distribution is obtained by Barrett-Joyner-Halenda (BJH) method and displayed in Fig. 5b. Compared to the original Co_3O_4, larger pores can be found in Co_3O_4-AC, demonstrating the acidic treatment can still affect the physical structure of the original Co_3O_4 to a certain extent. From Table 2, it can be seen that the average pore size becomes larger and the pore volume decreases over the acidic treated Co_3O_4, which means the original pores have been enlarged by the etching effect of acidic treatment.

Fig. 6 shows a bundle-like morphology of the as-prepared Co_3O_4, similar to previous report [42,52,53]. Each Co_3O_4 bundle is assembled by several microrods with a length of 5–15 μm and the microrod is composed of aggregates of numerous nanoparticles which generate many irregular pores. Due to the thermally driven contraction process during the thermal decomposition of oxalate precipitants accompanied with the release of gas components (e.g. CO_2 and H_2O), it is easy to form porous structure as observed in many reports [42,54,55]. With acidic treatment, the bundle-like morphologies retained with the microrod units of smaller size and the nanoparticles on the microrod become sparser, indicating the original Co_3O_4 is partially dissolved by the acid solution and some inner-connection is destroyed. This might be a main reason for the decrease of surface area after acidic treatment. In TEM images of Fig. 7, the porous microrod aggregated with numerous nanoparticles can be clearly observed. For original Co_3O_4 catalyst, the average size of nanoparticles with smooth edge is about 10–20 nm and a randomly selected nanoparticle (Fig. 6c) has the (220) crystal plane with lattice spacing of 0.29 nm. Compared to the original particles, the edge of the Co_3O_4-AC nanoparticles becomes much rougher which can be ascribed to the formation of crystal defect like steps during the acidic treatment. More surface defects may provide sufficient active sites for oxidation reactions which may contribute to the much improved activity in Co_3O_4-AC over the original one.

H_2-TPR and O_2-TPD analyses were carried out to investigate the surface chemistry of as-prepared catalysts as shown in Fig. 8. After hydrogen reducing treatment, both Co_3O_4-original and Co_3O_4-AC have shown two main reduction peaks in the temperature ranges of 200–300 °C and 300–500 °C, respectively. The first peak below 300 °C can be attributed to the reduction of Co_3O_4 into CoO and the higher one belongs to the reduction of CoO in to metallic Co [12,30,31,56]. The reduction peak at high temperature exhibits a clear asymmetrical characteristic due to the diverse reduction of surface oxygen and deep-interior oxygen defects, and more obvious peak shoulders can be found on the Co_3O_4-AC sample, suggesting more active surfaces after acidic treatment. Compared to the reducibility of original Co_3O_4, the acid-treated one also has a lower reduction temperature, further demonstrating the promotion effect of acid treatment. Meanwhile, the hydrogen consumption can be calibrated by doing H_2-TPR process of standard CuO sample and carrying on peak fitting of H_2-TPR profiles, and the results are shown in Figs. S4 and S5 . As shown in Table 2, the hydrogen consumption for low-temperature (< 350 °C) reduction on the Co_3O_4-AC sample is clearly higher than that value of original one, demonstrating that there are more active oxygen species on the Co_3O_4-AC sample. For O_2-TPD analysis, the result is very meaningful as shown in Fig. 8b. Under inert atmosphere, the different oxygen species on Co_3O_4 will desorb from the easiest to the hardest. Surface chemisorbed oxygen species (O_2^-, O^- and O_2^{2-}) will be easier to desorb from transitional metal oxides, which are also considered as the surface-active surface oxygen and can be utilized as well as recycled during catalytic reactions [30,57,58]. On the other hand, the lattice oxygen will be difficult to desorb because of the strong bonding in the crystal structure. In Fig. 8b, several desorption peaks can be observed such as

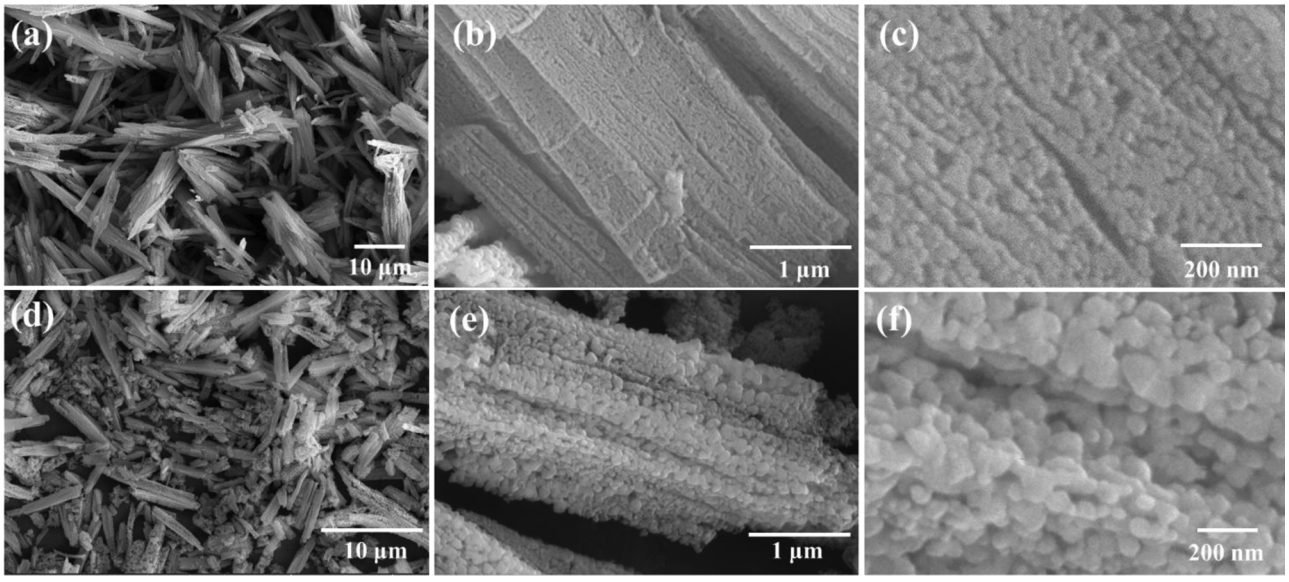

Fig. 6. SEM images of (a–c) Co_3O_4-original and (d–f) Co_3O_4-AC catalysts.

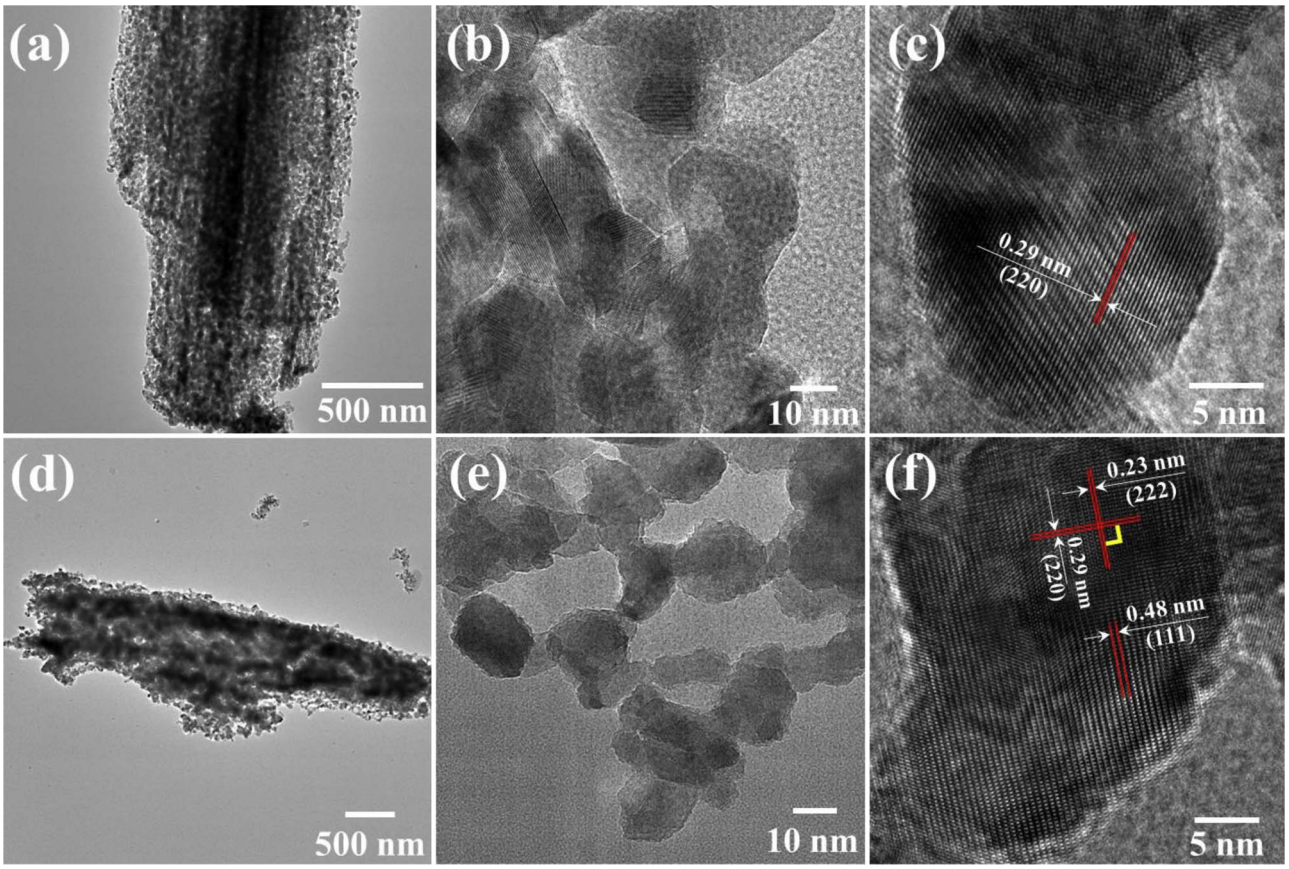

Fig. 7. TEM and HR-TEM images of (a–c) Co_3O_4-original and (d–f) Co_3O_4-AC catalysts.

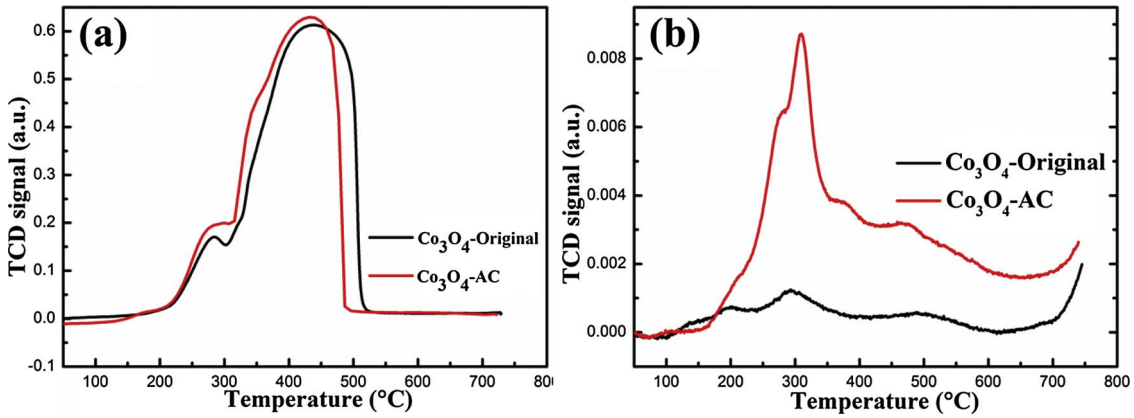

Fig. 8. H_2-TPR (a) and O_2-TPD (b) patterns of Co_3O_4-original and Co_3O_4-AC catalysts.

peaks below 350 °C, between 350 and 500 °C and above 700 °C, which can be ascribed to surface chemisorbed oxygen, surface lattice oxygen and interior phase lattice oxygen, respectively [19,30,59]. The Co_3O_4-AC sample clearly presented clear desorption peaks for low-temperature processes below 350 °C, with a peak intensity much greater than that for original Co_3O_4, suggesting a higher defective oxygen population on the surface of Co_3O_4-AC catalyst. Therefore, acidic treatment on cobalt oxide can effectively create abundant surface lattice defects and result in more chemisorbed oxygen species, resulting improved catalytic activities.

Fig. 9a shows the full XPS spectrum of the as-prepared Co_3O_4, which confirms the presence of Co and O in both samples. In addition, the Na 1s spectra peak appears clearly in the original Co_3O_4 as depicted in Fig. 9b, indicating the presence of Na on its surface. The surface Na species might be due to the usage of sodium oxalate during the synthetic process. But over the acidic treated sample, no peak attributed to Na was detected, demonstrating the surface Na was removed during the acid treatment. Moreover, high-resolution Co 2p3/2 and O1s spectral regions of both samples were shown in Fig. 9c and d, respectively. The Co 2p3/2 peak can be deconvoluted into two peaks by a peak-fitting deconvolution technique: biding energy at 779.3 and 780.8 eV, which can be assigned to the surface Co^{3+} and Co^{2+} species, respectively [12,13,30,57]. As listed in Table 2, the Co^{2+}/Co^{3+} ratio of Co_3O_4-AC is 1.44 much bigger than the value of Co_3O_4-original (0.45), indicating the acidic treatment significantly reduces the population of Co^{3+} while increases the population of Co^{2+} simultaneously. Using a similar deconvoluting method, the asymmetrical O1s peak can be fitted with three components: lattice oxygen (O^{2-}) at about 528.2 and 529.3 eV; chemisorbed oxygen species (O_2^-, O^- and O_2^{2-}) at 530.5 eV; adsorbed molecular water or hydroxyl group at 532.5 eV. The

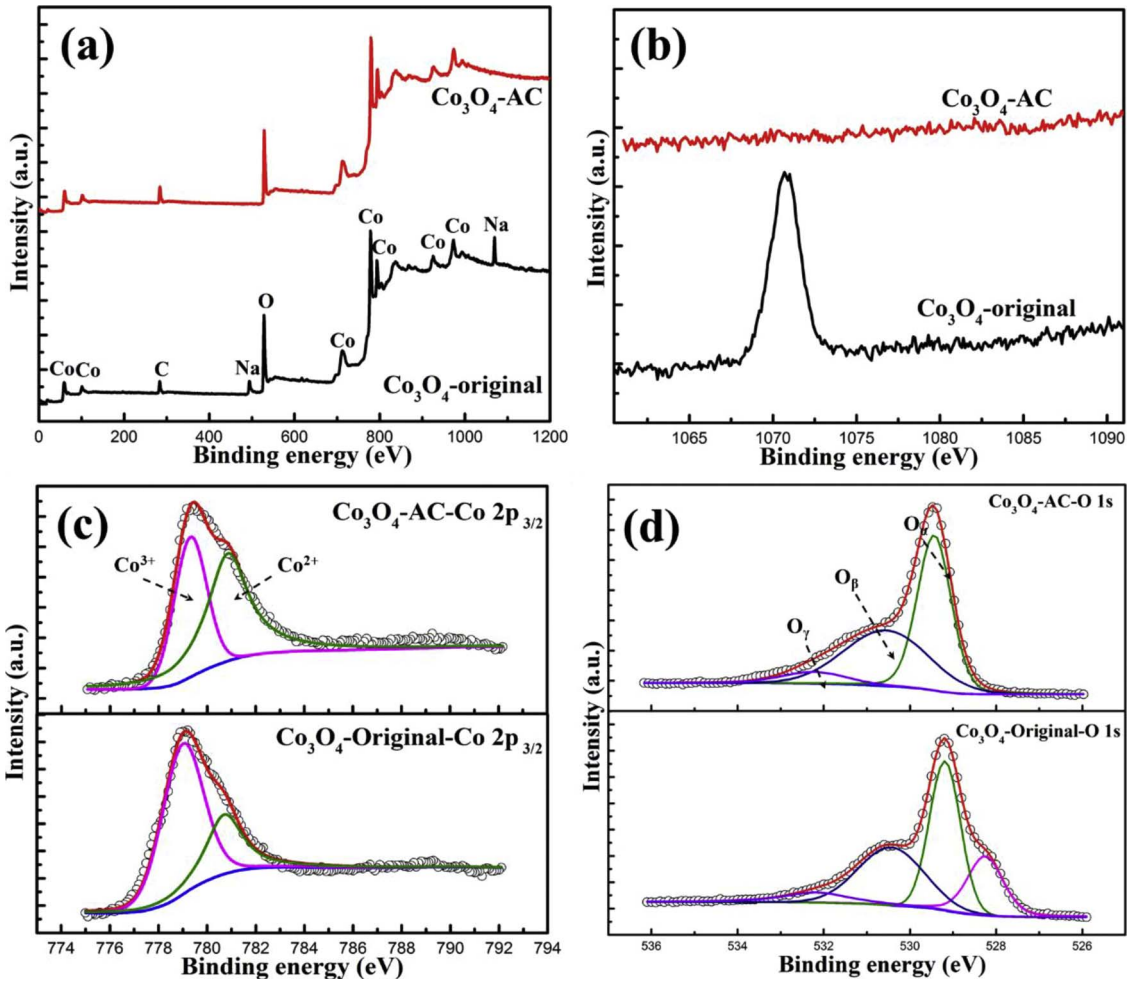

Fig. 9. XPS spectra of Co_3O_4-original and Co_3O_4-AC catalysts: (a) Full spectrum; (b) Na1s; (c) Co $2p_{3/2}$; (d) O 1s.

shoulder peak observed at 528.2 eV might be due to the incorporation of Na into the spinel Co_3O_4. Generally, the mobility of chemisorbed oxygen species is better that of lattice oxygen, which will be more active in related oxidation reactions. With acidic treatment, the population of chemisorbed oxygen species on Co_3O_4-AC is significantly increased, leading to the enhanced catalytic activity.

3.3. Discussions

In the past few years, porous structure-derived surface area has been used as a factor for tailoring the oxidation activities of metal oxides based catalysts [25,30,33,55]. Typically resulting from smaller pore sizes, higher surface area is expected to provide more surface-active sites for catalytic reactions. On the contrary, in this study the surface area of cobalt oxide decreased from 27.9 to 22.3 $m^2 g^{-1}$ after acidic treatment while the catalytic activity was significantly promoted. It seems that the surface area may not be a critical parameter in catalytic propane combustion, as reported previously [60,61]. However, due to the irregularity of special pores, significant surface defects such as steps and kinks can be observed on the porous materials to be beneficial to catalytic reactions. TEM results show that the original Co_3O_4 particles have relatively smooth surface while acidic treatment made the edge of Co_3O_4 nanoparticles rougher due to the formation of abundant surface crystal defects such as steps and kinks. With the acidic treatment, surface oxygen species were partly reacted with protons, and then cobalt species were selectively dissolved into the solution, giving rise to the rough surface with populated surface crystal defects in Co_3O_4 nanoparticles.

Sodium has been detected in the original Co_3O_4 samples as shown in XPS result, which can be due to the incorporation into oxalate precursor during the synthetic process. According to the previous studies [62–71], both promoting and inhibition effect can be observed through different catalytic reactions. For deNO_x selective catalytic reduction (SCR) catalysts, alkali metals such as Na and K are a major concern in commercial SCR catalysts as they may clog the pores of the catalyst channel and poison the catalyst by reacting with the active sites [62,63]. However, alkali metals can also significantly promote the activity of metal oxides based catalyst for NO/N_2O decomposition [64,65,71], soot oxidation [69,72] and formaldehyde oxidation [50,67]. In NO/N_2O decomposition, the addition of trace alkali metals may weaken Co—O bond strength and promote oxygen desorption from Co_3O_4 as well as be beneficial for generating surface NO_2^- species, which will further react with the adsorbed NO species to form N_2 [65,73]. However, in this study, it seems that the sodium in Co_3O_4 has a negative effect on catalytic combustion of propane. With acidic treatment, the surface sodium has been removed as confirmed by XPS result, while the propane oxidation activity was greatly enhanced. It is still not clear how the sodium species affect activity of Co_3O_4 in hydrocarbon oxidation, which is in need of further research.

In Co_3O_4 spinel structure, two cobalt species Co^{2+} and Co^{3+} occupy the tetrahedral sites and octahedral sites, respectively. XPS results show the much higher population of surface Co^{2+} of acid-treated Co_3O_4 than that on the original one, indicating more oxygen vacancies were generated by acidic treatment on Co_3O_4. This result was also confirmed by the analysis of O1s XPS, and the ratio of surface defect oxygen species to surface lattice oxygen (O_β/O_α) is 0.835 on Co_3O_4-AC, which is much

higher than the original value (0.549). Moreover, the O_2-temperature-programmed desorption (TPD) measurements provided auxiliary evidence for the better oxygen mobility on Co_3O_4-AC. The intensity of O_2-TPD peak for Co_3O_4-AC is much higher than that for original Co_3O_4, demonstrating there are more active oxygen species to be available during the catalytic reactions. For hydrocarbon (propane, propylene and methane etc.) oxidations, oxygen vacancies in metal oxides like CeO_2, Co_3O_4, MnO_2 and perovskite play a vital role in catalytic oxidation reactions [14,74,75]. Under oxygen-rich reaction condition, oxygen will prefer to be adsorbed on the oxygen vacancy sites and the dissociation will take place to generate active oxygen species to allow the oxidation of hydrocarbon. Therefore, the activity for catalytic combustion of propane over Co_3O_4 can be significantly promoted by simple acidic treatment which can make more surface crystal defects, generate higher ratio of surface Co^{2+}/Co^{3+} and O_β/O_α as well as give rise to better oxygen mobility.

4. Conclusion

In conclusion, a simple acidic treatment was developed for boosting the catalytic activity of Co_3O_4 in propane combustion. With this facile treatment, the novel Co_3O_4 exhibited more surface crystal defects, larger population of Co^{2+} and surface chemisorbed oxygen species, as well as better oxygen mobility. It is suggested both the surface physical structure and defect chemistry were modified, giving rise to an outstanding catalytic activity on propane combustion. Over this novel Co_3O_4 catalyst, the temperature of 90% propane conversion can take place at 250 °C under ultra-high WHSV (240 000 ml g^{-1} h^{-1}), which is 150, 118, 85 °C lower than that over the original Co_3O_4 catalyst and the commercial 1%Pt (or Pd)/Al_2O_3 as well as self-made 1%Pt (or Pd)/CeO_2 catalysts, respectively. Compared to the commercial Pt (or Pd)/Al_2O_3 and self-made 1%Pt (or Pd)/CeO_2, the etched Co_3O_4 structures not only have a much higher propane oxidation activity under low temperature and high space velocity, but also exhibits high stability and excellent water and sulfur resistance, as well as keeps a high conversion value with varying oxygen and propane concentrations. This chemical leaching strategy offers a promising approach for boosting the catalytic activities of oxides based materials in heterogeneous reactions.

Acknowledgements

The authors are grateful for the financial support from the US Department of Energy (Award No. DE-EE0006854) and the US National Science Foundation (Award No. CBET-1344792).

Appendix A. Supplementary data

Supplementary data associated with this article can be found, in the online version, at https://doi.org/10.1016/j.apcatb.2017.12.075.

References

[1] H.-H. Yang, L.-T. Hsieh, H.-C. Liu, H.-H. Mi, Atmos. Environ. 39 (2005) 17–25.
[2] K. Ravindra, R. Sokhi, R. Van Grieken, Atmos. Environ. 42 (2008) 2895–2921.
[3] R. Derwent, M. Jenkin, S. Saunders, Atmos. Environ. 30 (1996) 181–199.
[4] V. Ramaswamy, O. Boucher, J. Haigh, D. Hauglustaine, J. Haywood, G. Myhre, T. Nakajima, G. Shi, S. Solomon, R.E. Betts, Radiative Forcing of Climate Change, Pacific Northwest National Laboratory (PNNL), Richland, WA (US), 2001.
[5] R. Prasad, P. Singh, Catal. Sci. Technol. 3 (2013) 3223–3233.
[6] R. Opat, Y. Ra, R. Krieger, R.D. Reitz, D.E. Foster, R.P. Durrett, R.M. Siewert, Investigation of mixing and temperature effects on HC/CO emissions for highly dilute low temperature combustion in a light duty diesel engine, SAE Technical Paper, (2007).
[7] J.J. Spivey, Ind. Eng. Chem. Res. 26 (1987) 2165–2180.
[8] H. Huang, Y. Xu, Q. Feng, D.Y. Leung, Catal. Sci. Technol. 5 (2015) 2649–2669.
[9] C.P. O'Brien, I.C. Lee, J. Catal. 347 (2017) 1–8.
[10] A.S. Ivanova, E.M. Slavinskaya, R.V. Gulyaev, V.I. Zaikovskii, O.A. Stonkus, I.G. Danilova, L.M. Plyasova, I.A. Polukhina, A.I. Boronin, Appl. Catal. B: Environ. 97 (2010) 57–71.
[11] C.P. O'Brien, G.R. Jenness, H. Dong, D.G. Vlachos, I.C. Lee, J. Catal. 337 (2016) 122–132.
[12] Z. Zhu, G. Lu, Z. Zhang, Y. Guo, Y. Guo, Y. Wang, ACS Catal. 3 (2013) 1154–1164.
[13] Z. Ren, Z. Wu, W. Song, W. Xiao, Y. Guo, J. Ding, S.L. Suib, P.-X. Gao, Appl. Catal. B: Environ. 180 (2016) 150–160.
[14] W. Zhang, L. Hu, F. Wu, J. Li, Catal. Lett. 147 (2017) 407–415.
[15] Y. Xie, Y. Guo, Y. Guo, L. Wang, W. Zhan, Y. Wang, X. Gong, G. Lu, RSC Adv. 6 (2016) 50228–50237.
[16] Y. Xie, Y. Yu, X. Gong, Y. Guo, Y. Guo, Y. Wang, G. Lu, CrystEngComm 17 (2015) 3005–3014.
[17] H.J. Choi, J. Moon, H.B. Shim, K.S. Han, E.G. Lee, K.D. Jung, J. Am. Ceram. Soc. 89 (2006) 343–345.
[18] S. Pengpanich, V. Meeyoo, T. Rirksomboon, K. Bunyakiat, Appl. Catal. A: Gen. 234 (2002) 221–233.
[19] L. Liotta, M. Ousmane, G. Di Carlo, G. Pantaleo, G. Deganello, G. Marcì, L. Retailleau, A. Giroir-Fendler, Appl. Catal. A: Gen. 347 (2008) 81–88.
[20] J.-Y. Luo, M. Meng, Y.-Q. Zha, L.-H. Guo, J. Phys. Chem. C 112 (2008) 8694–8701.
[21] B. Faure, P. Alphonse, Appl. Catal. B: Environ. 180 (2016) 715–725.
[22] M. Alifanti, J. Kirchnerova, B. Delmon, D. Klvana, Appl. Catal. A: Gen. 262 (2004) 167–176.
[23] N.A. Merino, B.P. Barbero, P. Ruiz, L.E. Cadús, J. Catal. 240 (2006) 245–257.
[24] W. Si, Y. Wang, Y. Peng, J. Li, Angew. Chem. 127 (2015) 8065–8068.
[25] W. Si, Y. Wang, S. Zhao, F. Hu, J. Li, Environ. Sci. Technol. 50 (2016) 4572–4578.
[26] W. Si, Y. Wang, Y. Peng, X. Li, K. Li, J. Li, Chem. Commun. 51 (2015) 14977–14980.
[27] Y. Peng, W. Si, J. Luo, W. Su, H. Chang, J. Li, J. Hao, J. Crittenden, Environ. Sci. Technol. 50 (2016) 6442–6448.
[28] Z. Ren, Y. Guo, Z. Zhang, C. Liu, P.-X. Gao, J. Mater. Chem. A 1 (2013) 9897–9906.
[29] X. Xie, Y. Li, Z.-Q. Liu, M. Haruta, W. Shen, Nature 458 (2009) 746–749.
[30] B. Bai, H. Arandiyan, J. Li, Appl. Catal. B: Environ. 142–143 (2013) 677–683.
[31] W. Tang, Y. Deng, W. Li, S. Li, X. Wu, Y. Chen, Catal. Commun. 72 (2015) 165–169.
[32] C. Zhang, Y. Guo, Y. Guo, G. Lu, A. Boreave, L. Retailleau, A. Baylet, A. Giroir-Fendler, Appl. Catal. B 148 (2014) 490–498.
[33] S. Xie, J. Deng, S. Zang, H. Yang, G. Guo, H. Arandiyan, H. Dai, J. Catal. 322 (2015) 38–48.
[34] W. Si, Y. Wang, S. Zhao, F. Hu, J. Li, Environ. Sci. Technol. 50 (2016) 4572–4578.
[35] B. Solsona, T.E. Davies, T. Garcia, I. Vázquez, A. Dejoz, S.H. Taylor, Appl. Catal. B: Environ. 84 (2008) 176–184.
[36] R.P. Marin, S.A. Kondrat, R.K. Pinnell, T.E. Davies, S. Golunski, J.K. Bartley, G.J. Hutchings, S.H. Taylor, Appl. Catal. B: Environ. 140 (2013) 671–679.
[37] Q. Liu, L.-C. Wang, M. Chen, Y. Cao, H.-Y. He, K.-N. Fan, J. Catal. 263 (2009) 104–113.
[38] T. Garcia, S. Agouram, J.F. Sánchez-Royo, R. Murillo, A.M. Mastral, A. Aranda, I. Vázquez, A. Dejoz, B. Solsona, Appl. Catal. A: Gen. 386 (2010) 16–27.
[39] W. Zhang, F. Wu, J. Li, Z. You, Appl. Surf. Sci. 411 (2017) 136–143.
[40] M.S.L. Aparicio, I.D. Lick, React. Kinet. Mech. Catal. 119 (2016) 469–479.
[41] N. Rezlescu, E. Rezlescu, P.D. Popa, C. Doroftei, M. Ignat, Appl. Catal. B: Environ. 158 (2014) 70–75.
[42] P. Alphonse, Appl. Catal. B: Environ. 180 (2016) 715–725.
[43] Y. Xie, Y. Guo, Y. Guo, L. Wang, W. Zhan, Y. Wang, X.q. Gong, G. Lu, Catal. Sci. Technol. 6 (2016) 8222–8233.
[44] I.Y. Pakharukov, A.Y. Stakheev, I.E. Beck, Y.V. Zubavichus, V.Y. Murzin, V.N. Parmon, V.I. Bukhtiyarov, ACS Catal. 5 (2015) 2795–2804.
[45] C. Kokkofitis, M. Stoukides, J. Catal. 243 (2006) 428–437.
[46] A.D. Mayernick, M.J. Janik, J. Catal. 278 (2011) 16–25.
[47] K.B. Kim, M.K. Kim, Y.H. Kim, K.S. Song, E.D. Park, Res. Chem. Intermed. 36 (2010) 603–611.
[48] Y. Lou, J. Ma, X. Cao, L. Wang, Q. Dai, Z. Zhao, Y. Cai, W. Zhan, Y. Guo, P. Hu, ACS Catal. 4 (2014) 4143–4152.
[49] P.P. Rodenbough, C. Zheng, Y. Liu, C. Hui, Y. Xia, Z. Ran, Y. Hu, S.W. Chan, J. Am. Ceram. Soc. 100 (2017) 384–392.
[50] B. Bai, J. Li, ACS Catal. 4 (2014) 2753–2762.
[51] I. Lopes, N. El Hassan, H. Guerba, G. Wallez, A. Davidson, Chem. Mater. 18 (2006) 5826–5828.
[52] W. Tang, W. Li, D. Li, G. Liu, X. Wu, Y. Chen, Catal. Lett. 144 (2014) 1900–1910.
[53] L. Gao, S. Xu, C. Xue, Z. Hai, D. Sun, Y. Lu, J. Nanopart. Res. 18 (2016) 1–10.
[54] W. Tang, X. Wu, D. Li, Z. Wang, G. Liu, H. Liu, Y. Chen, J. Mater. Chem. A 2 (2014) 2544.
[55] W. Tang, Y. Deng, W. Li, J. Li, G. Liu, S. Li, X. Wu, Y. Chen, Catal. Sci. Technol. 6 (2016) 1710–1718.
[56] W. Tang, X. Wu, S. Li, W. Li, Y. Chen, Catal. Commun. 56 (2014) 134–138.
[57] B. Bai, J. Li, ACS Catal. 4 (2014) 2753–2762.
[58] W. Tang, M. Yao, Y. Deng, X. Li, N. Han, X. Wu, Y. Chen, Chem. Eng. J. 306 (2016) 709–718.
[59] Y.-Z. Wang, Y.-X. Zhao, C.-G. Gao, D.-S. Liu, Catal. Lett. 125 (2008) 134–138.
[60] L. Hu, Q. Peng, Y. Li, J. Am. Chem. Soc. 130 (2008) 16136–16137.
[61] F. Wang, H. Dai, J. Deng, G. Bai, K. Ji, Y. Liu, Environ. Sci. Technol. 46 (2012) 4034–4041.
[62] Å. Kling, C. Andersson, Å. Myringer, D. Eskilsson, S.G. Järås, Appl. Catal. B: Environ. 69 (2007) 240–251.
[63] D. Nicosia, I. Czekaj, O. Kröcher, Appl. Catal. B: Environ. 77 (2008) 228–236.
[64] C. Ohnishi, K. Asano, S. Iwamoto, K. Chikama, M. Inoue, Catal. Today 120 (2007) 145–150.
[65] M. Haneda, Y. Kintaichi, N. Bion, H. Hamada, Appl. Catal. B: Environ. 46 (2003) 473–482.
[66] C. Zhang, F. Liu, Y. Zhai, H. Ariga, N. Yi, Y. Liu, K. Asakura, M. Flytzani-Stephanopoulos, H. He, Angew. Chem. Int. Ed. 51 (2012) 9628–9632.
[67] Y. Huang, W. Fan, B. Long, H. Li, W. Qiu, F. Zhao, Y. Tong, H. Ji, J. Mater. Chem. A

4 (2016) 3648–3654.
[68] Y. Zhai, D. Pierre, R. Si, W. Deng, P. Ferrin, A.U. Nilekar, G. Peng, J.A. Herron, D.C. Bell, H. Saltsburg, Science 329 (2010) 1633–1636.
[69] E. Aneggi, C. de Leitenburg, G. Dolcetti, A. Trovarelli, Catal. Today 136 (2008) 3–10.
[70] L. Xue, H. He, C. Liu, C. Zhang, B. Zhang, Environ. Sci. Technol. 43 (2009) 890–895.
[71] P. Stelmachowski, G. Maniak, A. Kotarba, Z. Sojka, Catal. Commun. 10 (2009) 1062–1065.
[72] T. Jakubek, W. Kaspera, P. Legutko, P. Stelmachowski, A. Kotarba, Catal. Commun. 71 (2015) 37–41.
[73] M. Haneda, Y. Kintaichi, H. Hamada, Appl. Catal. B: Environ. 55 (2005) 169–175.
[74] J.M. López, A.L. Gilbank, T. García, B. Solsona, S. Agouram, L. Torrente-Murciano, Appl. Catal. B: Environ. 174 (2015) 403–412.
[75] N.D. Wasalathanthri, A.S. Poyraz, S. Biswas, Y. Meng, C.-H. Kuo, D.A. Kriz, S.L. Suib, J. Phys. Chem. C 119 (2015) 1473–1482.